



## Original article

Nanna Bjerregaard Pedersen, Jeannette Jacqueline Łucejko\*, Francesca Modugno and Charlotte Björdal

# Correlation between bacterial decay and chemical changes in waterlogged archaeological wood analysed by light microscopy and Py-GC/MS

<https://doi.org/10.1515/hf-2020-0153>

Received June 3, 2020; accepted October 16, 2020;  
published online November 20, 2020

**Abstract:** Erosion bacteria are the main degraders of archaeological wood excavated from waterlogged environments. Light microscopy and analytical pyrolysis coupled with gas chromatography/mass spectrometry (Py-GC/MS) were exploited to study waterlogged archaeological wood (*Pinus sylvestris* L.) at different stages of bacterial decay. The research explored the biochemical changes related to erosion bacteria degradation of the secondary cell wall in the wood cells and the chemical changes related to abiotic processes induced by the long-term waterlogged burial environment. Erosion bacteria were demonstrated by chemical analysis to cause significant holocellulose depletion. Detailed analysis of the holocellulose and lignin pyrolysis products revealed only minor chemical changes in the residual structure even after heavy erosion bacteria decay. Chemical changes in the lignin polymer is associated to enzymatic unlocking of the lignocellulose to gain access to the holocellulose fraction of the cell wall. Chemical changes in the holocellulose fraction are suggested to stem from depolymerisation and from alterations in the polymer matrix of the residual wood cell wall structure. Interestingly, a difference was observed between the sound reference wood and the waterlogged

archaeological wood without erosion bacteria decay, indicating that long-term exposure in waterlogged environments results in partial decay of the holocellulose even in absence of bacterial activity.

**Keywords:** archaeological wood; erosion bacteria; holocellulose; light microscopy; lignin; Py(HMDS)-GC/MS.

## 1 Introduction

Archaeological wooden artefacts, like shipwrecks, built heritage, and objects of everyday use are in some cases capable of being preserved for centuries when buried in anoxic waterlogged environments. Archaeologists recover remarkable wooden finds from the past from peats, wetlands, marine sediments and clay soils where wood is protected from aggressive wood degrading fungi, insects, and wood boring mussels. However, archaeological wood material presents a typical soft and spongy-like surface layer, although the integrity and physical shape appears preserved. These striking features are closely related to bacterial degradation of the secondary cell wall (Björdal 2012). Erosion bacteria decay is the most common form of decay in waterlogged archaeological wood in near anaerobic environments (Björdal et al. 1999; Klaassen 2008). The decay starts at the wood surface and proceeds slowly inwards. The low decay rate entails that the waterlogged wooden artefacts often feature an evident gradient of decay from the surface to the core: presence of morphologically well-preserved wood cells in the inner parts of the wood material, and of heavily decayed cells in the surface layer of the same fragment. Detailed morphological studies of erosion bacteria decay have shown similar decay patterns in a wide range of different wood species and waterlogged environments (Björdal et al. 1999; Blanchette et al. 1990; Huisman et al. 2008; Kim et al. 2000). At the cell wall level, erosion bacteria preferentially degrade the holocellulose-rich secondary cell wall, resulting in a remaining fragile wood skeleton mainly composed of the lignin-rich middle

**\*Corresponding author: Jeannette Jacqueline Łucejko**, Department of Chemistry and Industrial Chemistry, University of Pisa, Pisa, Italy, E-mail: jeannette.lucejko@unipi.it. <https://orcid.org/0000-0002-7717-4039>

**Nanna Bjerregaard Pedersen**, Royal Danish Academy, Institute for Conservation, Copenhagen, Denmark, E-mail: nbje@kglakademi.dk. <https://orcid.org/0000-0002-5744-939X>

**Francesca Modugno**, Department of Chemistry and Industrial Chemistry, University of Pisa, Pisa, Italy, E-mail: francesca.modugno@unipi.it. <https://orcid.org/0000-0002-0446-668X>

**Charlotte Björdal**, Department of Marine Sciences, University of Gothenburg, Gothenburg, Sweden

lamella and amorphous residual material filling the cell lumen (Björkdal et al. 2000; Kim et al. 1996; Pedersen et al. 2015; Pedersen et al. 2014; Singh et al. 1991). Today the biochemical pathway for anaerobic wood decay by erosion bacteria is not fully understood, as the identity of the specific bacteria has not yet been established. Attempts to isolate and grow monocultures with traditional microbiological methods have failed (Nilsson et al. 2008a; Nilsson et al. 2008b; Nilsson et al. 2008c; Schmidt et al. 1995; Schmidt et al. 1987). Laboratory experiments suggest that erosion bacteria are facultative anaerobes bacteria and part of a bacterial consortia (Kretschmar et al. 2008; Nilsson et al. 2008b). Landy et al. (2008) reported that erosion bacteria most likely fall within the Cytophaga-Flavobacterium-Bacteroides sub-group, on the basis of DNA analysis on sub-cultured bacterial isolates, and of DNA extracted from erosion bacterial degraded wood. During decay, erosion bacteria are closely attached to the wood matrix by multi-enzyme complexes (cellulosomes) (Björkdal et al. 2000; Holt et al. 1983; Singh et al. 1991; Singh et al. 1990). This is a common energy saving strategy of anaerobic bacteria (Bayer et al. 2008).

Considering the inadequacy of the identification of erosion bacteria detailed chemical analysis of the decay pattern can point to possible biochemical pathways of the bacteria and likewise give more detailed knowledge on the chemical composition of the remaining wood material - something very important for development of proper conservation treatments. Chemical imaging techniques are potentially highly effective for the chemical analysis of individual cell wall layers *in situ* (Fackler et al. 2013). However, only very few studies have focused on waterlogged wood (Čufar et al. 2008; McQueen et al. 2019; Pedersen et al. 2015; Pedersen et al. 2014), and some are limited to the mapping of elements derived from inorganic components within the wood structure (McQueen et al. 2017). Spatially resolved chemical information on lignocellulosic polymers was obtained using confocal Raman imaging and UV-micro spectrophotometry on waterlogged archaeological *Picea abies* (L.) H. Karst. solely decayed by erosion bacteria. The results showed a high degree of lignin preservation in the residual wood structure, accompanied by a significant degradation of polysaccharides (Pedersen et al. 2015). The residual material from the secondary cell wall contained lignin, with a strong depletion of carbohydrates. Based on the spectral data, the chemical composition of the lignin resulted similar to the lignin of the secondary cell wall in sound waterlogged material, indicating that lignin is not affected by the biochemical decay process of erosion bacteria. However, in morphologically sound areas (not bacterial degraded) of *P. abies*, from the

same wood material submerged under (near) anoxic conditions for approximately 400 years, spectral analyses indicated possible minor abiotic hydrolysis and oxidation of the lignin polymer (Pedersen 2015; Pedersen et al. 2015; Pedersen et al. 2014). Abiotic decay of wood in waterlogged submerging environments has rarely been studied, but waterlogged wood with intact micro-morphology has been found to show signs of slight holocellulose (cellulose and hemicelluloses) depolymerisation and chemical changes in the lignin-carbohydrate complex (Borgin et al. 1975; Gelbrich et al. 2008; Pedersen et al. 2015).

The high spatial resolution of chemical imaging has improved the knowledge of the chemical composition and distribution of macromolecules in waterlogged wood. However, the methods lack high chemical resolution. As described above, analytical techniques have been widely used for the chemical characterisation of waterlogged wood deterioration, but in general the interpretation of the results are limited, because most studies do not define the decay type or the degree of degradation prior to analysis (Pedersen et al. 2013).

Analytical pyrolysis combined with gas chromatography and mass spectrometry (Py-GC/MS) has proven to be a powerful technique for the chemical characterisation of high molecular weight organic materials in complex matrices, on the basis of the GC/MS determination of the qualitative and quantitative profile of pyrolysis products, which are small volatile molecules produced by thermal degradation of the sample (Bonaduce et al. 2016; Degano et al. 2018).

When wood is analysed by Py-GC/MS, selective bond cleavage of wooden polymers, cellulose, hemicellulose and lignin, is induced by providing thermal energy to the sample (Moldoveanu 1998a). This technique has achieved semi-quantitative results at a complex macromolecular level, with a high degree of chemical detail thanks to detailed analysis of the categorized lignin and polysaccharides pyrolysis products (Alves et al. 2006; Fabbri et al. 2001; Łucejko et al. 2018b; Moldoveanu 2010; Tamburini et al. 2014; Zoia et al. 2017).

Analytical pyrolysis (Py-GC/MS) is able to highlight the chemical changes that occurred both in the lignin and in the polysaccharides of the wood. It allowed to observe the depletion and depolymerization of polysaccharides and side chain shortening, oxidation or demethylation processes that occurred in the lignin polymer in wood (Łucejko et al. 2018b; Romagnoli et al. 2018; Tamburini et al. 2017; Zoia et al. 2017). Py-GC/MS is also highly sensitive, requires a small amount of sample (50–100 µg) without any pre-treatment. Absence of pre-treatment avoids the risks of chemically altering the wood polymers prior to analyses, as

would be the case if polymer separation by gravimetric analysis were used. These technical features are highly desirable in the heritage science field (Degano et al. 2018). The use of 1,1,1,3,3,3-hexamethyldisilazane (HMDS) as silylating agent increases the yield of compounds bearing OH groups. Furthermore, this derivatizing agent, actively participating in the pyrolysis process protects the hydroxyl functionalities present in the pyrolysis products by generating partially silylated compounds and by promoting base-catalysed thermal degradations, such as dehydration (Fabbri et al. 2001; Fabbri et al. 2002; Fabbri et al. 2003).

This study presents the investigation of the chemical alteration of lignocellulosic polymers in a waterlogged archaeological wooden pole of Scots pine affected by erosion bacteria decay at different levels. The aim of this work is a contribution to understand and distinguish the biochemical changes related to erosion bacteria degradation of the secondary cell wall in the wood cells and the chemical changes related to abiotic processes induced by the long-term waterlogged burial environment. This was accomplished by analysis performed by analytical pyrolysis (Py-GC/MS) of samples with varying degree of erosion bacteria decay, carefully selected after morphological examination by aid of light microscope.

## 2 Materials and methods

### 2.1 Materials

A waterlogged archaeological pole ( $\varnothing = 100$  mm) from a well construction dated to the 17–18th century and made from Scots pine (*Pinus sylvestris* L.) was used in this study. The pole was in a very good state of preservation without any visible dehydration damage or collapse. The surface layer was soft and spongy, whereas the inner parts remained hard and seemingly sound. The pole was excavated in Nibe (Denmark) in the summer of 2010 by the Historical Museum of Northern Jutland, Denmark, and stored in anoxic water prior to analysis. The reference dry heartwood material of *P. sylvestris* came from of a modern 99-year old sound tree from the Gołębki Forest District, near Biskupin (Poland) (Zborowska et al. 2007).

### 2.2 Light microscopy and retrieval of samples for chemical analyses

An approximately 2 cm thick disc was sawn from the archaeological pole. One radial slice was removed by knife and hammer from the surface towards the centre. The slice was examined by light microscopy in order to assess that the wood was solely degraded by erosion bacteria and that areas of different degree of decay were available for chemical analysis. First, subsamples

(approximately  $3 \times 3 \times 20$  mm) were systematically taken along the length of the slice. From each subsample thin transversal and longitudinal sections were cut by hand with a double-edged razor blade and stained with either 0.1% w/v safranin O in 50% ethanol or 0.1% aniline blue in 50% lactic acid. Finally, the sections were investigated by light microscopy and polarized light, at magnification of up to 630 times.

It was concluded that the wood material fulfilled the experimental demands and from the systematic investigation of the subsamples three areas were selected with different degree of decay for chemical analyses. These were: (1) xylem heavily decayed by erosion bacteria from the outer part of the pole (EB-heavy), (2) undecayed xylem from the inner part of the pole (EB-non), and (3) xylem partly decayed by erosion bacteria located between the surface and the core (EB-partly). The degree of decay EB heavy, EB-non, EB-partly are comparable to the classification “total disintegration”, “absent”, and “moderate”, respectively (Klaassen 2008). The three selected waterlogged archaeological wood samples and the reference material (approximately  $0.5 \text{ cm}^3$ ) were oven-dried for 24 h at 40–50 °C, ball milled (Pulverisette 23, Fritsch GmbH, Germany) and divided into three replica samples each: Ref1, Ref2, Ref3, EB-heavy1, EB-heavy2, EB-heavy3, EB-partly1, EB-partly2, EB-partly3, EB-non1, EB-non2, and EB-non3, thus prepared, they were analysed by analytical pyrolysis.

### 2.3 Py-GC/MS

Analytical pyrolysis was performed in the presence of 1,1,1,3,3,3-hexamethyldisilazane (HMDS, chemical purity 99.9%, Sigma Aldrich Inc., USA). HMDS is a silylating agent for the in situ thermally assisted derivatisation of pyrolysis products.

Approximately 60  $\mu\text{g}$  of each replica sample were admixed with 3.0  $\mu\text{L}$  of HMDS directly into a stainless steel cup, and placed in the micro-furnace at a temperature of 550 °C of Multi-Shot Pyrolyzer EGA/Py-3030D (Frontier Lab) coupled with a gas chromatograph 6890 (Agilent Technologies, USA), and with a Agilent 5973 Mass Selective Detector operating in electron impact mode (EI) at 70 eV. The other instrumental condition of a system Py(HMDS)-GC/MS was described in (Łucejko et al. 2018a).

The pyrolysis products derived from the lignin and holl-cellulose were identified by comparing their mass spectra with spectra reported in the Wiley and NIST08 libraries and in the literature (Mattonai et al. 2016; McQueen et al. 2017; Tamburini et al. 2016). Automated Mass Spectral Deconvolution and Identification System software (AMDIS) was used to deconvolute and integrate the chromatographic peaks using a customised library containing the mass spectra of 150 compounds. Semi-quantitative calculations were conducted using chromatographic areas: peak areas were normalised with respect to the sum of the peak areas of all the pyrolysis products identified, and the data were averaged and expressed as percentages. The percentage areas were used to calculate the relative abundances of wood pyrolysis products divided into categories (listed in Table 1), based on their chemical structure as described in Tamburini et al., (Tamburini et al. 2015). The relative amounts of individual pyrolysis products were averaged for the three replicates analysed for each type of waterlogged material (EB-non, EB-partly, EB-heavy).

**Table 1:** Pyrolysis products obtained by Py(HMDS)-GC/MS of reference pine wood sample assigned into either origin (O): holocellulose (H) or lignin (L) polymers, and grouped into categories (c): furans (H-f), cyclopentenones (H-c), pyranones (H-p), anhydrosugars (H-a) hydroxybenzenes (H-h), monomers (L-m), short chain (L-s), long chain (L-l), carbonyl (L-c), acids (L-a) and demethoxylated (L-d).

N°	Compound	O-c	N°	Compound	O-c
1	2-hydroxymethylfuran (TMS)	H-f	33	1,4-dihydroxybenzene (2TMS)	H-h
2	phenol (TMS)		34	arabinofuranose (4TMS)	H-a
3	1-hydroxy-1-cyclopenten-3-one (TMS)	H-c	35	4-vinylguaiaicol (TMS)	L-s
4	3-hydroxymethylfuran (TMS)	H-f	36	<i>E</i> -2,3-dihydroxy-cyclopent-2-enone (2TMS)	H-c
5	<i>o</i> -cresol (TMS)		37	4-ethylcatechol (2TMS)	L-d
6	2-furancarboxylic acid (TMS)	H-f	38	3-hydroxy-2-(hydroxymethyl) cyclopenta-2,4-dienone (2TMS)	H-c
7	<i>m</i> -cresol (TMS)		39	eugenol (TMS)	L-l
8	2-hydroxy-1-cyclopenten-3-one (TMS)	H-c	40	3,5-dihydroxy-2-methyl-(4H)-pyran-4-one (2TMS)	H-p
9	<i>p</i> -cresol (TMS)		41	1,6-anhydro-beta-D-glucopyranose (TMS at position 4)	H-a
10	3-hydroxy-(2H)-pyran-2-one (TMS)	H-p	42	1,6-anhydro-beta-D-glucopyranose (TMS at position 2)	H-a
11	<i>Z</i> -2,3-dihydroxy-cyclopent-2-enone (TMS)	H-c	43	<i>Z</i> -isoeugenol (TMS)	L-l
12	<i>E</i> -2,3-dihydroxy-cyclopent-2-enone (TMS)	H-c	44	vanillin (TMS)	L-c
13	1,2-dihydroxybenzene (TMS)	H-h	45	1,2,3-trihydroxybenzene (3TMS)	H-h
14	3-hydroxy-(4H)-pyran-4-one (TMS)	H-p	46	<i>E</i> -isoeugenol (TMS)	L-l
15	5-hydroxy-2H-pyran-4(3H)-one (TMS)	H-p	47	1,4-anhydro-D-galactopyranose (2TMS)	H-a
16	2-hydroxymethyl-3-methyl-2-cyclopentenone (TMS)	H-c	48	1,6-anhydro-D-galactopyranose (2TMS)	H-a
17	1-hydroxy-2-methyl-1-cyclopenten-3-one (TMS)	H-c	49	2-hydroxymethyl-5-hydroxy-2,3-dihydro-(4H)-pyran-4-one (2TMS)	H-p
18	1-methyl-2-hydroxy-1-cyclopenten-3-one (TMS)	H-c	50	1,4-anhydro-D-glucopyranose (2TMS at position 2 and 4)	H-a
19	1,3-dihydroxyacetone (2TMS)		51	1,2,4-trihydroxybenzene (3TMS)	H-h
20	guaiaicol (TMS)	L-s	52	acetovanillone (TMS)	L-c
21	3-hydroxy-6-methyl-(2H)-pyran-2-one (TMS)	H-p	53	4-hydroxy benzoic acid (2TMS)	L-a
22	2-methyl-3-hydroxy-(4H)-pyran-4-one (TMS)	H-p	54	1,6-anhydro-beta-D-glucopyranose (2TMS at position 2 and 4)	H-a
23	2-methyl-3-hydroxymethyl-2-cyclopentenone (TMS)	H-c	55	1,4-anhydro-D-galactopyranose (3TMS)	H-a
24	2,3-dihydrofuran-2,3-diol (2TMS)	H-f	56	2,3,5-trihydroxy-4H-pyran-4-one (3TMS)	H-p
25	5-hydroxymethyl-2-furaldehyde (TMS)	H-f	57	1,6-anhydro-beta-D-glucopyranose (3TMS)	H-a
26	4-methylguaiaicol (TMS)	L-s	58	1,4-anhydro-D-glucopyranose (3TMS)	H-a
27	1,2-dihydroxybenzene (2TMS)	H-h	59	vanillic acid (2TMS)	L-a
28	2-hydroxymethyl-2,3-dihydropyran-4-one (TMS)	H-p	60	vanillylpropanol (2TMS)	L-l
29	1,4:3,6-dianhydro- $\alpha$ -D-glucopyranose (TMS)	H-a	61	<i>Z</i> -coniferyl alcohol (2 TMS)	L-m
30	<i>Z</i> -2,3-dihydroxy-cyclopent-2-enone (2TMS)	H-c	62	coniferylaldehyde (TMS)	L-c
31	4-methylcatechol (2TMS)	L-d	63	<i>E</i> -coniferyl alcohol (2 TMS)	L-m
32	4-ethylguaiaicol (TMS)	L-s	64	3,4-dihydroxy cinnamyl alcohol (3TMS)	L-d

## 3 Results and discussion

### 3.1 Morphological decay pattern

Investigations on the waterlogged wood material by light microscopy showed a morphological decay pattern typical for erosion bacteria decay (Björdal et al. 2000; Björdal et al. 1999). Other types of wood decay patterns were not observed. This indicates that the microbiological decay solely derived from the activity of erosion bacteria. The most heavily degraded tracheids were observed in the exterior parts of the pile (Figure 1c) while sound undegraded tracheids were observed in the interior parts close to the pith (Figure 1a). A mixture of degraded and sound tracheids were observed in the xylem between the surface and core (Figure 1b). This shows that the waterlogged wood material contained a gradient of decay from

surface to core, as expected on the basis of previous descriptions of erosion bacteria decay processes in piles (Klaassen 2008; Macchioni et al. 2013). The decayed tracheids were characterized by an eroded secondary cell wall, and intact compound middle lamella, and cell corners. Residual cell wall material was left as an amorphous substance that reduced the cell lumen region or in some instances even filled up the whole cell lumen (Figure 1b). Totally disintegrated xylem consisted of a fragile skeleton of the compound middle lamella filled up by this residual material (Figure 1c).

The samples selected for Py-GC/MS chemical analysis represented three different stages of decay and thereby three samples with very different material characteristics. Sample “EB-non” had a morphologically sound xylem without any erosion bacteria decay signs. This indicates that any chemical modification observed in “EB-non”



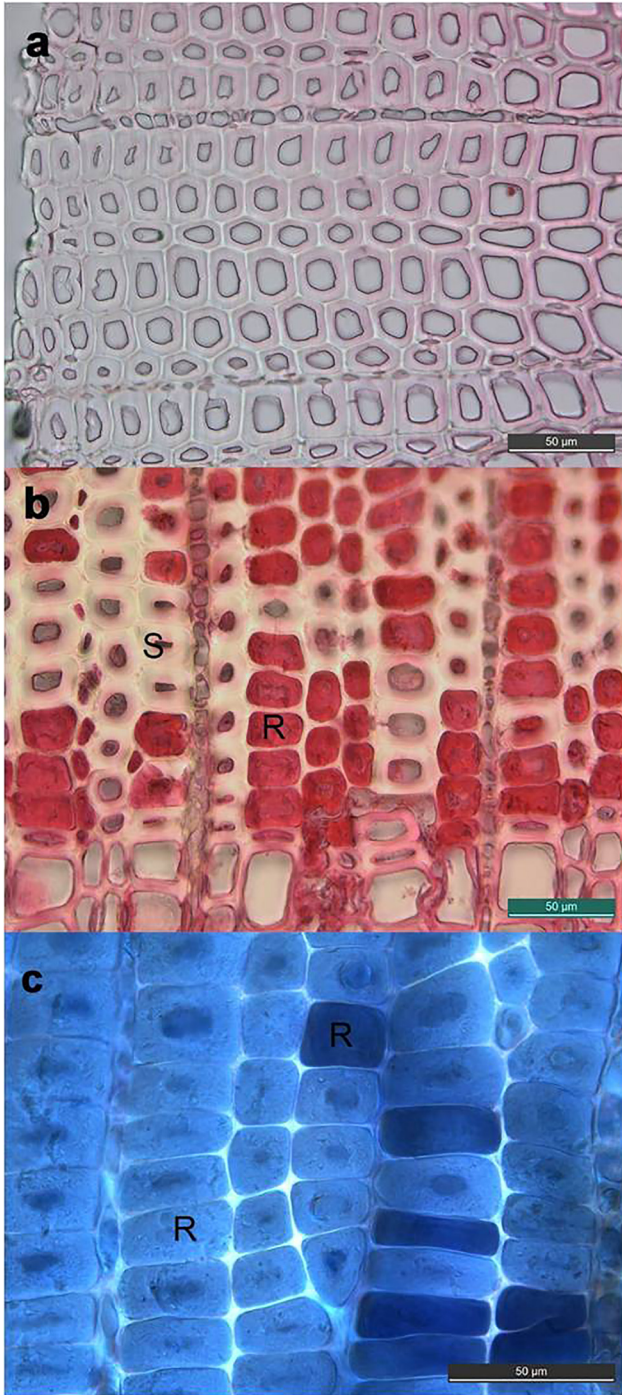


**Figure 1:** Light microscope cross sections of the waterlogged *Pinus sylvestris* pole. (a) Morphological intact secondary cell walls with no trace of erosion bacteria decay. (b) Intermediate erosion bacteria decay showing a mixture of morphologically sound tracheids (S) and tracheids with secondary cell wall decay leaving an amorphous residual material in the cell lumen (R). (c) Total secondary cell wall decay by erosion bacteria, the secondary cell wall of all tracheids are filled with typical residual material of erosion bacteria (R).

compared to the reference material is solely due to abiotic hydrolysis and possible oxidation induced by water, inorganic ions and organic acids during the long period of waterlogging. Sample “EB-heavy” contained xylem with complete degradation of the secondary cell walls, leaving only a fragile skeleton of the compound middle lamella and residual material from the degradation of the secondary cell wall. Sample “EB-partly” contained a mixture of tracheids with degraded and un-degraded secondary cell walls. Sample “EB-heavy” and “EB-partly” is thus expected to contain chemical signatures both from microbial erosion bacteria decay and from abiotic decay due to the submerging environment.

## 3.2 Py-GC/MS analysis

### 3.2.1 Pyrolysis products

Analytical pyrolysis coupled with GC-MS was applied to the archaeological waterlogged wood samples (“EB-non”, “EB-partly” and “EB-heavy”) and the reference sample. The pyrograms for the reference and the waterlogged pole samples with different degree of decay showed both holocellulose (cellulose and hemicelluloses) and lignin pyrolysis products with high abundances (Figure 2). Pyrolysis profiles of the waterlogged pole showed the same pyrolysis products as for the reference, but in different relative amounts. Since the same analytical conditions were used for all the samples, the different relative abundances obtained were the result of the changes undergone by the

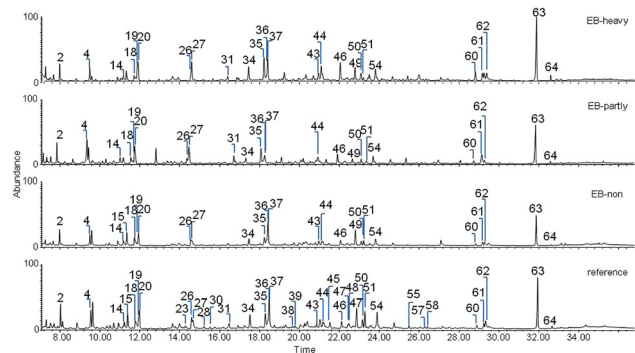


**Figure 2:** Pyrolysis profiles obtained for sound *Pinus sylvestris* (reference) and for the waterlogged *P. sylvestris* samples of the outer heavily decayed xylem (EB-heavy), the partly decayed xylem (EB-partly), and the inner morphological intact xylem (EB-non). Numbers refer to pyrolysis product peak listed in Table 1.

material at the molecular level, which influenced the relative yields of the pyrolytic processes (Tamburini et al. 2017). In fact, the differences in the relative abundances of pyrolysis products between the waterlogged samples (Figure 2), indicating that molecular changes in the lignocellulosic cell wall material is related to the gradient of decay in the waterlogged wood (Tamburini et al. 2017; Zoia et al. 2017). A total of 64 pyrolysis products from the reference material were identified and assigned to either holocellulose (H) or lignin (L). Table 1 lists the identified pyrolysis products of sound reference *P. sylvestris* together with the assigned category of holocellulose as furans (H-f), pyrans (H-p), cyclopentenones (H-c), hydroxybenzenes (H-h) and anhydrosugars (H-a) and lignin as monomers (L-m), short chain (L-s), long chain (L-l), carbonyl (L-c), demethylated (L-d) and acids (L-a).

### 3.2.2 Holocellulose/lignin ratios

The ratio H/L is generally measured by gravimetric analysis and used for internal comparison of a data set (Babiński et al. 2019; Giachi et al. 2003; Tamburini et al. 2015). Previous studies have shown that the pyrolytic H/L ratio also provides a reliable and comparable estimation (Łucejko et al. 2012). For this reason, the pyrolytic holocellulose versus lignin ratio (H/L) was calculated as the ratio between the sum of the peak areas of holocellulose pyrolysis products ( $\Sigma H$ ) and the lignin pyrolysis products ( $\Sigma L$ ) (Table 2). This index is recognised as a powerful parameter for determining the extent of degradation of waterlogged wood, which is usually characterized by the loss of polysaccharides, therefore an decrease in H/L is observed when compared with sound undegraded wood (Huang et al. 2013; Łucejko et al. 2015; Łucejko et al. 2012). This semi-quantitative calculations highlighted that the waterlogged sample “EB-non” had undergone a loss of holocellulose of about 6% (H/L  $2.2 \pm 0.2$ ), confirming its very good state of preservation, whereas the loss of holocellulose for “EB-partly” and “EB-heavy” was much higher as expected, leading to low

or very low H/L ratios ( $1.0 \pm 0.2$  and  $0.6 \pm 0.1$ , respectively).

The lower value of the H/L ratio of waterlogged but morphological sound wood (“EB-non”, H/L  $2.2 \pm 0.2$ ) compared to the reference sound wood (H/L  $2.7 \pm 0.1$ ) shows that abiotic degradation of the holocellulose fraction most likely occurred. This indicates presence of chemical alteration in the lignocellulosic matrix not accompanied by morphologically altered structure detectable with light microscopy. The results obtained for “EB-partly” and “EB-heavy” confirm that erosion bacteria decay leads to a considerable depletion of carbohydrates, and that the depletion of holocellulose occurred to a higher degree in the surface layer of the pole that was heavily decayed by erosion bacteria (EB-heavy) than in the partly decayed xylem closer to the pith, which contained a higher proportion of un-decayed cell wall material (EB-partly). This is in agreement with results reported in the literature on chemical alteration induced by erosion bacteria decay (Pedersen et al. 2013). The H/L ratio gives an overall picture of carbohydrate depletion and lignin conservation but does not provide any information on the specific chemical changes that occurred in the wood polymers. However, molecular information can be obtained by examining the relative amounts of categorised pyrolysis products in more detail.

### 3.2.3 Changes in the chemical composition of holocellulose

A limitation of the analytical pyrolysis method is that it does not permit differentiating the pyrolysis products of cellulose and hemicelluloses, as the thermal degradation process form the same pyrolysis products from the two types of polymers. This means that the method cannot reveal details of chemical changes observed specifically in cellulose and hemicelluloses but will refer to chemical changes occurring in the overall polysaccharide (holocellulose) fraction of the wood samples. Pyrolysis products formed during the thermal degradation of holocellulose were classified into five categories: cyclopentenones, furans, pyranones hydroxybenzenes and anhydrosugars, according to (Moldoveanu 1998a; Pouwels et al. 1989; Ramirez-Corredores 2013). The sum of the peak areas assigned to each category (Table 1) were expressed as a percentage of the total abundance of holocellulose pyrolysis products in each sample (Figure 3a).

A comparison of the relative distributions of categorised holocellulose pyrolysis products shows difference between the reference pine and waterlogged

**Table 2:** Average relative percentage of holocellulose (H) and lignin (L) pyrolysis products in the analyzed wood material obtained for three replicas.

Scots pine	Sound	Waterlogged archaeological wood		
	Reference	EB-non	EB-partly	EB-heavy
Sum H	$72.7 \pm 0.4$	$68.6 \pm 2.2$	$48.3 \pm 5.1$	$34.8 \pm 2.3$
Sum L	$27.3 \pm 0.4$	$31.4 \pm 2.2$	$51.7 \pm 5.1$	$65.2 \pm 2.3$
H/L	$2.7 \pm 0.1$	$2.2 \pm 0.2$	$1.0 \pm 0.2$	$0.6 \pm 0.1$

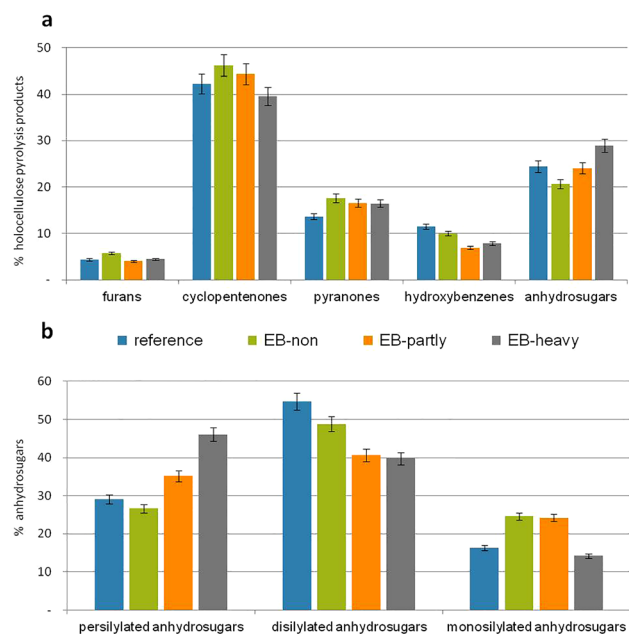


**Figure 3:** Percentage distribution of (a) holocellulose pyrolysis product grouped into categories, calculated in relation to the total amount of holocellulose in each sample; (b) anhydrosugars from the holocellulose pyrolysis products with three different degrees of silylation calculated in relation to the total amount of anhydrosugars in each sample. The values are based on analyses of three replicas for each sample. Whiskers show the standard deviation of the replica measurements.

samples, and as expected also within the waterlogged wood samples with different degree of bacterial decay (Figure 3a).

In particular, sample “EB-non” that is not attacked by bacteria and morphologically similar to the reference sound wood, presents a distribution profile of holocellulose pyrolysis products different from that of sound wood. This indicates that certain chemical changes in the carbohydrate polymers take place due to permanence in the waterlogged anoxic environment as abiotic decay in absence of bacterial activity. This is in agreement with the few available chemical analyses of morphological sound waterlogged wood performed in earlier studies (Borgin et al. 1975; Gelbrich et al. 2008; Pedersen et al. 2015).

A notable chemical difference relates to the categories of anhydrosugars and cyclopentenones. An increase in the relative abundances of anhydrosugars and decrease in cyclopentenones can be related to depolymerisation of polysaccharides (Tamburini et al. 2017). In this case the relative amount of anhydrosugars is lower in “EB-non” than in the reference. This indicates a lower amount of low molecular polysaccharides in “EB-non” than in the reference. This can be explained by microbial removal of easily accessible and degradable non-structural carbohydrates

like starch stored in parenchyma cells and maybe also by removal of depolymerised structural carbohydrates from the wood structure due to abiotic physical and chemical processes in the waterlogged burial environment. After removal of small fragments, oligomers, and monomers the residual carbohydrates have a lower level of depolymerisation, resulting in a lower pyrolysis yield of anhydrosugars and higher of cyclopentenones.

Differences in the relative amount of cyclopentenones and anhydrosugars between the waterlogged wood samples is related to a higher relative amount of anhydrosugars (from 21 to 29%) and lower amount of cyclopentenones (from 46 to 40%) with increase in erosion bacteria decay (Figure 3a). Levoglucosan is the most abundant compound found in the group of anhydrosugars (Table 1), and its abundance can be related to the degree of polymerization of cellulose. Moldoveanu (1998b) reported that cellulose with a degree of polymerization (DP) of more than 200 generated about 20% levoglucosan during pyrolysis while cellulose with DP less than 200 formed 44% more levoglucosan. This confirms that erosion bacteria depolymerise the polysaccharides fraction of the cell wall.

The chemical differences in the pyrolytic profiles of the holocellulose fractions (Figure 3), are not pronounced compared to the distinctive anatomical changes in the material (Figure 1). This is probably due to the fact that erosion bacteria consume the polysaccharide fraction of the secondary cell wall without leaving residual sugars during and after decay as suggested by Pedersen et al. (2015). The cell wall is either decayed by erosion bacteria or sound; confirming that erosion bacteria has very close contact to the cell wall during decay and very effectively utilise all available sugars. The result thereby suggest that heavily decayed waterlogged wood contains intact holocellulose only in the morphologically sound compound middle lamella that is not degraded by erosion bacteria due to its high content of lignin.

The distribution profile of anhydrosugars with different degree of silylation formed during pyrolysis and shown in Figure 3b. Three types of silylated anhydrosugars can be formed depending on the number of OH groups that have reacted with the silylating agent (HMDS) to create the corresponding trimethylsilyl ester: monosilylated, disilylated, or persilylated (three -OTMS groups) (Figure 3b). The degree of silylation of anhydrosugars gives an indication of the reactivity of the hydroxyl groups in terms of their hydrogen exchange with the TMS groups. The reaction is not quantitative due to steric hindrance, but the less the anhydrosugars are derivatised during pyrolysis, the tighter the holocellulose polymers are bound in the cell wall polymer network (Evershed 1993; Fabbri et al. 2003).



In the reference wood samples, the disilylated form prevails. The reference and “EB-non” samples are similar in the relative distribution of their derivatised anhydrosugars. This is in good agreement with the morphological similarity between the two material types. With increased erosion bacteria decay (“EB-partly” and “EB-heavy”), persilylated anhydrosugars become more abundant while disilylated anhydrosugars decrease. In “EB-partly” the amount of persilylated anhydrosugars are almost equal to the amount of disilylated anhydrosugars; in “EB-heavy” the amount of persilylated anhydrosugars are higher than the amount of disilylated anhydrosugars. This can either be explained by a partly unwinding of the cell wall polymer matrix during decay or by the difference in ultrastructure of un-decayed cell wall material left in the decayed wood material. The remaining holocellulose in “EB-heavy” is located in the primary cell wall of the compound middle lamella, whereas a high portion of the holocellulose in “EB-non” and “EB-partly” is located in the secondary cell walls. The cellulose in the primary cell wall is arranged in thin crossing layers embedded in pectin, whereas the cellulose and hemicelluloses of the secondary cell wall are arranged in a highly organised parallel structure (Abe et al. 2005). It is possible that the less ordered structure of the cellulose fibrils - or the higher amount of pectin present in the primary cell wall - has an effect in the difference in the relative distribution of silylated anhydrosugars.

### 3.2.4 Changes in chemical composition of lignin

Gymnosperms such as *P. sylvestris* contain lignin composed almost entirely of guaiacyl and small quantities of p-hydroxyphenyl units. The lignin pyrolysis products were divided into five categories according to their molecular structure (Huang et al. 2014; Kawamoto et al. 2008; Kotake et al. 2013; Kotake et al. 2014; Tamburini et al. 2015): *Z*- and *E*- coniferyl alcohols **monomers**, **short** side **chain** guaiacyl units, **long** side **chain** guaiacyl units, **oxidised** guaiacyl units with carbonyl and carboxyl functional groups, and **demethylated** guaiacyl units (Table 1). Variations between the relative amounts of these categories in the different types of wood material were observed (Figure 4a). This indicates chemical alterations in the lignin polymer.

Chemical changes between sound reference wood and the morphologically sound waterlogged archaeological sample (EB-non) suggest abiotic decay as a consequence of the immersion in the waterlogged environment. The most pronounced difference in the lignin profile of these two samples is that the relative abundance of demethylated units (pyrolysis products) in the waterlogged wood is less than half of that of the sound wood (Figure 4a). Demethylation of lignin moieties in the waterlogged wood have been reported previously (Pedersen et al. 2013). This study shows that 200–300 years of burial in a waterlogged environment significantly affects the decrease of this type of functional group in the lignin polymer. The second

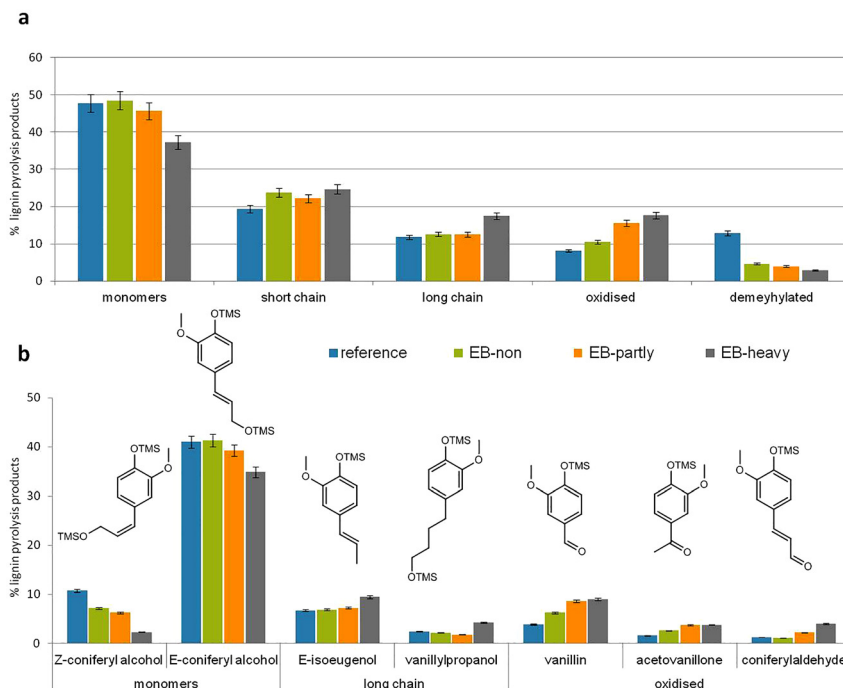


**Figure 4:** Percentage distribution of (a) lignin pyrolysis products grouped into categories; (b) selected individual lignin pyrolysis products. All values calculated in relation to the total amount of lignin in each sample and based on analyses of three replicates of each sample. Whiskers show the standard deviation of the replicates. TMS-trimethylsilyl group.



distinct difference in relative amounts of pyrolysis products between reference sample and “EB-non” is the increase in the number of oxidised units, and the slight increase in short chain pyrolysis products (Figure 4a). These changes can suggest that the lignin polymer has undergone an alteration due to abiotic decay during the waterlogging period.

Chemical changes between the morphologically sound waterlogged archaeological sample (EB-non) and waterlogged wood decayed by erosion bacteria (“EB-partly” and “EB-heavy”) consist of relatively small changes in chemical composition of lignin compared to the great difference in the morphology. This indicates that the composition of the lignin polymer network is only slightly affected by the action of erosion bacteria. The chemical differences consist of a slight decrease in demethylated guaiacyl units, a decrease in coniferyl alcohols monomers, an increase in long side chain guaiacyl units, and an increase in oxidised guaiacyl units (Figure 4a). The decrease in the relative abundance of coniferyl alcohols (*Z*- and *E*- monomers) in the pyrolysis profile is directly related to the increase in the degree of erosion bacteria decay and is pronounced for both monomers, whereas the increase in long side chain units are most pronounced for vanillylpropanol and *E*-isoeugenol (Figure 4b). The changes observed in the lignin polymer indicate an alteration in the propanoid side chains, probably due to cleavage of the bonds and oxidation of some positions (Zoia et al. 2017) due to the erosion bacteria activity.

Oxidised guaiacyl units primarily stem from formation of guaiacyl units containing carbonyl and carboxyl functionalities in the alkyl side chain at the  $\alpha$ -position, which are conjugated with the aromatic ring (Figure 4b) (Crestini et al. 2003; Tarabanko et al. 2017).

A slight depolymerisation, demethylation and oxidation of the lignin polymer are, by the design of this study, linked to erosion bacteria decay. This is a novel finding, although not surprising, as the erosion bacteria in some way need to rearrange the cell wall, and thereby the lignin polymer, to reach the “encapsulated” polymeric carbohydrates within the micro fibrils of the cell wall as these are their essential nutrient. This alteration of lignin was not reported in Raman imaging investigations (Pedersen et al. 2015). The oxidation induced by bacteria primarily results in the formation of guaiacyl units containing carbonyl functionalities in the alkyl side chain, vanillin, acetovanillone and coniferylaldehyde (Figure 4b). In particular, erosion bacteria oxidation leads to the preferential formation of aldehyde functional groups at the  $\gamma$ -position of the coniferyl alcohol monomers.

## 4 Conclusions

Combined morphological and chemical investigation of waterlogged archaeological *P. sylvestris* gave new insight to the chemical composition and changes that takes place during decay by erosion bacteria.

Erosion bacteria cause a massive holocellulose depletion and thereby have a great impact on the quantitative chemical composition, the morphology and the physical properties of the wood material. Detailed study of the holocellulose fraction show, despite the great morphological changes, only minor alterations related to depolymerisation and hydroxyl bonding capacity. This indicates that the cell wall is either decayed or intact; the carbohydrate degradation by erosion bacteria is highly effective in terms of utilisation of all carbohydrate cell wall material.

The study suggest that erosion bacteria induces minor changes in the lignin structure, which enable them to access and efficiently degrade the holocellulose. In addition, it was observed that solely abiotic chemical changes of both lignin and holocellulose takes place as a consequence of long-term exposure in a waterlogged anoxic environment in wood that is not exposed to bacterial activity.

**Acknowledgements:** The authors would like to thank The Historical Museum of Northern Jutland, Denmark and Hanne Billeschou Juhl from Bevaringscenter Nord, Denmark for saving and sharing the waterlogged wood material.

**Author contribution:** All the authors have accepted responsibility for the entire content of this submitted manuscript and approved submission.

**Research funding:** This work was supported by the Fund for basic research activities FFABR 2017, The Ministry of Education, University and Research (MIUR), Italy and University of Pisa research project PRA\_2018\_26 “Advanced analytical pyrolysis to study polymers in renewable energy, environment, cultural heritage”.

**Conflict of interest statement:** The authors declare no conflicts of interest.

## References

- Abe, H. and Funada, R. (2005). Review: the orientation of cellulose microfibrils in the cell walls of tracheids in conifers. *IAWA J.* 26: 161–174.
- Alves, A., Schwanninger, M., Pereira, H., and Rodrigues, J. (2006). Analytical pyrolysis as a direct method to determine the lignin content in wood part 1: comparison of pyrolysis lignin with Klason lignin. *J. Anal. Appl. Pyrolysis* 76: 209–213.

- Babiński, L., Zborowska, M., Fabisiak, E., and Prądzyński, W. (2019). Are the wooden remains of the Lusitanian culture settlement at Biskupin safe? Decomposition of archaeological oak wood samples during a 10-year experiment. *Archaeol. Anthropol. Sci.* 11: 6583–6594.
- Bayer, E.A., Henrissat, B., and Lamed, R. (2008). The cellulosome: a natural bacterial strategy to combat biomass recalcitrance. In: *Biomass recalcitrance: deconstructing the plant cell wall for bioenergy*, pp. 407–435, <https://doi.org/10.1002/9781444305418.ch13>.
- Björdal, C.G. (2012). Microbial degradation of waterlogged archaeological wood. *J. Cult. Herit.* 13: S118–S122.
- Björdal, C.G., Nilsson, T., and Daniel, G.F. (1999). Microbial decay of waterlogged archaeological wood found in Sweden applicable to archaeology and conservation. *Int. Biodeterior. Biodegrad.* 43: 63–73.
- Björdal, C.G., Daniel, G., and Nilsson, T. (2000). Depth of burial, an important factor in controlling bacterial decay of waterlogged archaeological poles. *Int. Biodeterior. Biodegrad.* 45: 15–26.
- Blanchette, R.A., Nilsson, T. and Daniel, G.F. (1990). Biological degradation of wood. In: Rowell, R.M. and Barbour, R.J. (Eds.), *Archaeological wood: properties, chemistry, and preservation*. Washington: American Chemical Society, pp. 141–174.
- Bonaduce, I., Ribechini, E., Modugno, F., and Colombini, M.P. (2016). Analytical approaches based on gas chromatography mass spectrometry (GC/MS) to study organic materials in artworks and archaeological objects. *Top. Curr. Chem.* 374: 6.
- Borgin, K., Parameswaran, N., and Liese, W. (1975). The effect of aging on the ultrastructure of wood. *Wood Sci. Technol.* 9: 87–98.
- Crestini, C. and Tagliatesta, P. (2003). 66: metalloporphyrins in the biomimetic oxidation of lignin and lignin model compounds: development of alternative delignification strategies. In: Kadish, K.M., Smith, K.M., and Guillard, R. (Eds.), *The porphyrin handbook*. Amsterdam: Academic Press, pp. 161–203.
- Čufar, K., Gričar, J., Zupančič, M., Koch, G., and Schmitt, U. (2008). Anatomy, cell wall structure and topochemistry of water-logged archaeological wood aged 5,200 and 4,500 years. *IAWA J.* 29: 55–68.
- Degano, I., Modugno, F., Bonaduce, I., Ribechini, E., and Colombini, M.P. (2018). Recent advances in analytical pyrolysis to investigate organic materials in heritage science. *Angew. Chem. Int. Ed.* 57: 7313–7323.
- Evershed, R.P. (1993). Advances in silylation. In: Blau, K. and Halket, J. (Eds.), *Handbook of derivatives for chromatography*. New York: John Wiley & Sons, pp. 51–100.
- Fabbri, D. and Chiavari, G. (2001). Analytical pyrolysis of carbohydrates in the presence of hexamethyldisilazane. *Anal. Chim. Acta* 449: 271–280.
- Fabbri, D., Chiavari, G., Prati, S., Vassura, I., and Vangelista, M. (2002). Gas chromatography/mass spectrometric characterisation of pyrolysis/silylation products of glucose and cellulose. *Rapid Commun. Mass Spectrom.* 16: 2349–2355.
- Fabbri, D., Prati, S., Vassura, I., and Chiavari, G. (2003). Off-line pyrolysis/silylation of cellulose and chitin. *J. Anal. Appl. Pyrolysis* 68–69: 163–171.
- Fackler, K. and Thygesen, L.G. (2013). Microspectroscopy as applied to the study of wood molecular structure. *Wood Sci. Technol.* 47: 203–222.
- Gelbrich, J., Mai, C., and Miltz, H. (2008). Chemical changes in wood degraded by bacteria. *Int. Biodeterior. Biodegrad.* 61: 24–32.
- Giachi, G., Bettazzi, F., Chimichi, S., and Staccioli, G. (2003). Chemical characterisation of degraded wood in ships discovered in a recent excavation of the Etruscan and Roman harbour of Pisa. *J. Cult. Herit.* 4: 75–83.
- Holt, D.M. and Jones, E.B. (1983). Bacterial degradation of lignified wood cell walls in anaerobic aquatic habitats. *Appl. Environ. Microbiol.* 46: 722–727.
- Huang, Y.-B. and Fu, Y. (2013). Hydrolysis of cellulose to glucose by solid acid catalysts. *Green Chem.* 15: 1095–1111.
- Huang, J., Liu, C., Wu, D., Tong, H., and Ren, L. (2014). Density functional theory studies on pyrolysis mechanism of  $\beta$ -O-4 type lignin dimer model compound. *J. Anal. Appl. Pyrolysis* 109: 98–108.
- Huisman, D.J., Manders, M.R., Kretschmar, E.I., Klaassen, R.K.W.M., and Lamersdorf, N. (2008). Burial conditions and wood degradation at archaeological sites in The Netherlands. *Int. Biodeterior. Biodegrad.* 61: 33–44.
- Kawamoto, H., Ryoritani, M., and Saka, S. (2008). Different pyrolytic cleavage mechanisms of  $\beta$ -ether bond depending on the side-chain structure of lignin dimers. *J. Anal. Appl. Pyrolysis* 81: 88–94.
- Kim, Y.S. and Singh, A.P. (2000). Micromorphological characteristics of wood biodegradation in wet environments: a review. *IAWA J.* 21: 135–155.
- Kim, Y.S., Singh, A. P., and Nilsson, T. (1996). Bacteria as important degraders in waterlogged archaeological woods. *Holzforschung* 50: 389–392.
- Klaassen, R.K.W.M. (2008). Bacterial decay in wooden foundation piles — patterns and causes: a study of historical pile foundations in The Netherlands. *Int. Biodeterior. Biodegrad.* 61: 45–60.
- Kotake, T., Kawamoto, H., and Saka, S. (2013). Pyrolysis reactions of coniferyl alcohol as a model of the primary structure formed during lignin pyrolysis. *J. Anal. Appl. Pyrolysis* 104: 573–584.
- Kotake, T., Kawamoto, H., and Saka, S. (2014). Mechanisms for the formation of monomers and oligomers during the pyrolysis of a softwood lignin. *J. Anal. Appl. Pyrolysis* 105: 309–316.
- Kretschmar, E.I., Gelbrich, J., Miltz, H., and Lamersdorf, N. (2008). Studying bacterial wood decay under low oxygen conditions — results of microcosm experiments. *Int. Biodeterior. Biodegrad.* 61: 69–84.
- Landy, E.T., Mitchell, J.I., Hotchkiss, S., and Eaton, R.A. (2008). Bacterial diversity associated with archaeological waterlogged wood: ribosomal RNA clone libraries and denaturing gradient gel electrophoresis (DGGE). *Int. Biodeterior. Biodegrad.* 61: 106–116.
- Łucejko, J.J., Zborowska, M., Modugno, F., Colombini, M.P., and Pradzynski, W. (2012). Analytical pyrolysis vs. classical wet chemical analysis to assess the decay of archaeological waterlogged wood. *Anal. Chim. Acta* 745: 70–77.
- Łucejko, J.J., Modugno, F., Ribechini, E., Tamburini, D., and Colombini, M.P. (2015). Analytical instrumental techniques to study archaeological wood degradation. *Appl. Spectrosc. Rev.* 50: 584–625.
- Łucejko, J.J., La Nasa, J., McQueen, C.M.A., Braovac, S., Colombini, M.P., and Modugno, F. (2018a). Protective effect of linseed oil varnish on archaeological wood treated with alum. *Microchem. J.* 139: 50–61.
- Łucejko, J.J., Mattonai, M., Zborowska, M., Tamburini, D., Cofta, G., Cantisani, E., Kúdela, J., Cartwright, C., Colombini, M.P.,

- Ribechini, E., et al. (2018b). Deterioration effects of wet environments and brown rot fungus *Coniophora puteana* on pine wood in the archaeological site of Biskupin (Poland). *Microchem. J.* 138: 132–146.
- Macchioni, N., Capretti, C., Sozzi, L., and Pizzo, B. (2013). Grading the decay of waterlogged archaeological wood according to anatomical characterisation. The case of the Fivè site (N-E Italy). *Int. Biodeterior. Biodegrad.* 84: 54–64.
- Mattonai, M., Tamburini, D., Colombini, M.P., and Ribechini, E. (2016). Timing in analytical pyrolysis: Py(HMDS)-GC/MS of glucose and cellulose using online micro reaction sampler. *Anal. Chem.* 88: 9318–9325.
- McQueen, C.M.A., Tamburini, D., Łucejko, J.J., Braovac, S., Gambineri, F., Modugno, F., Colombini, M.P., and Kutzke, H. (2017). New insights into the degradation processes and influence of the conservation treatment in alum-treated wood from the Oseberg collection. *Microchem. J.* 132: 119–129.
- McQueen, C.M.A., Łucejko, J.J., Flåte, I.M.T., Modugno, F., and Braovac, S. (2019). Ammonium alum in alum-treated wooden artefacts: discovery, origins and consequences. *Heritage Science* 7: 78.
- Moldoveanu, S.C. (1998a). *Analytical pyrolysis of natural organic polymers*. Amsterdam: Elsevier Science.
- Moldoveanu, S.C. (1998b). Analytical pyrolysis of polymeric carbohydrates. In: Coleman, D. and Price, B.F. (Eds.), *Analytical pyrolysis of natural organic polymers*. Amsterdam: Elsevier Science, pp. 217–316.
- Moldoveanu, S.C. (2010). *Pyrolysis of organic molecules with applications to health and environment*. Oxford (UK): Elsevier.
- Nilsson, T. and Björdal, C. (2008a). Culturing wood-degrading erosion bacteria. *Int. Biodeterior. Biodegrad.* 61: 3–10.
- Nilsson, T. and Björdal, C. (2008b). The use of kapok fibres for enrichment cultures of lignocellulose-degrading bacteria. *Int. Biodeterior. Biodegrad.* 61: 11–16.
- Nilsson, T., Björdal, C., and Fällman, E. (2008c). Culturing erosion bacteria: procedures for obtaining purer cultures and pure strains. *Int. Biodeterior. Biodegrad.* 61: 17–23.
- Pedersen, N.B. (2015). *Microscopic and spectroscopic characterisation of waterlogged softwood from anoxic environments*, Ph.D. thesis. Copenhagen: University of Copenhagen.
- Pedersen, N.B., Björdal, C.G., Jensen, P., and Felby, C. (2013). Bacterial degradation of archaeological wood in anoxic waterlogged environments. In: Harding, S.E. (Ed.), *Stability of complex carbohydrate structures: biofuels, foods, vaccines and shipwrecks*: The Royal Society of Chemistry, pp. 160–187.
- Pedersen, N.B., Schmitt, U., Koch, G., Felby, C., and Thygesen, L.G. (2014). Lignin distribution in waterlogged archaeological *Picea abies* (L.) Karst degraded by erosion bacteria. *Holzforschung* 68: 791–798.
- Pedersen, N.B., Gierlinger, N., and Thygesen, L.G. (2015). Bacterial and abiotic decay in waterlogged archaeological *Picea abies* (L.) Karst studied by confocal Raman imaging and ATR-FTIR spectroscopy. *Holzforschung* 69: 103–112.
- Pouwels, A.D., Eijkel, G.B., and Boon, J.J. (1989). Curie-point pyrolysis-capillary gas chromatography-high-resolution mass spectrometry of microcrystalline cellulose. *J. Anal. Appl. Pyrolysis* 14: 237–280.
- Ramirez-Corredores, M.M. (2013). Chapter 6. Pathways and mechanisms of fast Pyrolysis: impact on catalyst research. In: Triantafyllidis, K., Lappas, A., and Stöcker, M. (Eds.), *The role of catalysis for the sustainable production of bio-fuels and bio-chemicals*. Amsterdam: Elsevier, pp. 161–216.
- Romagnoli, M., Vinciguerra, V., and Silvestri, A. (2018). Heat treatment effect on lignin and carbohydrates in Corsican pine earlywood and latewood studied by PY-GC-MS technique. *J. Wood Chem. Technol.* 38: 57–70.
- Schmidt, O., Nagashima, Y., Liese, W., and Schmitt, U. (1987). Bacterial wood degradation studies under laboratory conditions and in lakes. *Holzforschung* 41: 137–140.
- Schmidt, O., Moreth, U., and Schmitt, U. (1995). Wood degradation by a bacterial pure culture. *Mater. Org. (Berl.)* 29: 289–293.
- Singh, A.P. and Butcher, J.A. (1991). Bacterial degradation of wood cell walls: a review of degradation patterns. *Journal of the Institute of Wood Science* 12: 143–157.
- Singh, A.P., Nilsson, T., and Daniel, G.F. (1990). Bacterial attack of *Pinus sylvestris* wood under near-anaerobic conditions. *Journal of the Institute of Wood Science* 11: 237–249.
- Tamburini, D., Łucejko, J.J., Modugno, F., and Colombini, M.P. (2014). Characterisation of archaeological waterlogged wood from Herculaneum by pyrolysis and mass spectrometry, Part B. *Int. Biodeterior. Biodegrad.* 86: 142–149.
- Tamburini, D., Łucejko, J.J., Zborowska, M., Modugno, F., Prądzyński, W., and Colombini, M.P. (2015). Archaeological wood degradation at the site of Biskupin (Poland): wet chemical analysis and evaluation of specific Py-GC/MS profiles. *J. Anal. Appl. Pyrolysis* 115: 7–15.
- Tamburini, D., Łucejko, J.J., Ribechini, E., and Colombini, M.P. (2016). New markers of natural and anthropogenic chemical alteration of archaeological lignin revealed by in situ pyrolysis/silylation-gas chromatography-mass spectrometry. *J. Anal. Appl. Pyrolysis* 118: 249–258.
- Tamburini, D., Łucejko, J.J., Zborowska, M., Modugno, F., Cantisani, E., Mamoňová, M., and Colombini, M.P. (2017). The short-term degradation of cellulosic pulp in lake water and peat soil: a multi-analytical study from the micro to the molecular level. *Int. Biodeterior. Biodegrad.* 116: 243–259.
- Tarabanko, V.E. and Tarabanko, N. (2017). Catalytic oxidation of lignins into the aromatic aldehydes: general process trends and development prospects. *Int. J. Mol. Sci.* 18: 2421.
- Zborowska, M., Babiński, L., Gajewska, J., Waliszewska, B., and Prądzyński, W. (2007). Physical and chemical properties of contemporary pine wood (*Pinus sylvestris* L.) in conditions of a wet archaeological site in Biskupin. *Folia For. Pol.* 38: 13–26.
- Zoia, L., Tamburini, D., Orlandi, M., Łucejko, J.J., Salanti, A., Tolppa, E.-L., Modugno, F., and Colombini, M.P. (2017). Chemical characterisation of the whole plant cell wall of archaeological wood: an integrated approach. *Anal. Bioanal. Chem.* 409: 4233–4245.